polymers

MDPI

Article

Unravelling Main- and Side-Chain Motions in Polymers with NMR Spectroscopy and Relaxometry: The Case of Polyvinyl Butyral

Lucia Calucci [1,2], Silvia Pizzanelli [1,2,*], Alessandro Mandoli [3], Artur Birczyński [4], Zdzisław T. Lalowicz [5], Cristina De Monte [6], Lucia Ricci [6] and Simona Bronco [6]

1 Istituto di Chimica dei Composti OrganoMetallici, Consiglio Nazionale delle Ricerche—CNR, Via G. Moruzzi 1, 56124 Pisa, Italy; lucia.calucci@pi.iccom.cnr.it
2 Centro per l'Integrazione della Strumentazione Scientifica dell'Università di Pisa (CISUP), Lungarno Pacinotti 43/44, 56126 Pisa, Italy
3 Dipartimento di Chimica e Chimica Industriale, Università di Pisa, Via G. Moruzzi 13, 56124 Pisa, Italy; alessandro.mandoli@unipi.it
4 Institute of Technology, The Pedagogical University of Kraków, Podchorążych 2, 30-084 Krakow, Poland; artur.birczynski@ifj.edu.pl
5 Institute of Nuclear Physics, Polish Academy of Sciences, Ul. Radzikowskiego 152, 31342 Krakow, Poland; zdzislaw.lalowicz@ifj.edu.pl
6 Istituto per i Processi Chimico-Fisici, Consiglio Nazionale delle Ricerche—CNR, Via G. Moruzzi 1, 56124 Pisa, Italy; cristina.demonte@pi.ipcf.cnr.it (C.D.M.); lucia.ricci@pi.ipcf.cnr.it (L.R.); simona.bronco@pi.ipcf.cnr.it (S.B.)
* Correspondence: silvia.pizzanelli@pi.iccom.cnr.it; Tel.: +39-050-315-2549

Citation: Calucci, L.; Pizzanelli, S.; Mandoli, A.; Birczyński, A.; Lalowicz, Z.T.; De Monte, C.; Ricci, L.; Bronco, S. Unravelling Main- and Side-Chain Motions in Polymers with NMR Spectroscopy and Relaxometry: The Case of Polyvinyl Butyral. *Polymers* **2021**, *13*, 2686. https://doi.org/10.3390/polym13162686

Academic Editors: Carmelo Corsaro and Andrea Mele

Received: 18 June 2021
Accepted: 6 August 2021
Published: 11 August 2021

Publisher's Note: MDPI stays neutral with regard to jurisdictional claims in published maps and institutional affiliations.

Copyright: © 2021 by the authors. Licensee MDPI, Basel, Switzerland. This article is an open access article distributed under the terms and conditions of the Creative Commons Attribution (CC BY) license (http://creativecommons.org/licenses/by/4.0/).

Abstract: Polyvinyl butyral (PVB) is an amorphous polymer employed in many technological applications. In order to highlight the relationships between macroscopic properties and dynamics at a microscopic level, motions of the main-chain and of the propyl side-chains were investigated between T_g − 288 °C and T_g + 55 °C, with T_g indicating the glass transition temperature. To this aim, a combination of solid state Nuclear Magnetic Resonance (NMR) methods was applied to two purposely synthesized PVB isotopomers: one fully protonated and the other perdeuterated on the side-chains. ^{1}H time domain NMR and ^{1}H field cycling NMR relaxometry experiments, performed across and above T_g, revealed that the dynamics of the main-chain corresponds to the α-relaxation associated to the glass transition, which was previously characterized by dielectric spectroscopy. A faster secondary relaxation was observed for the first time and ascribed to side-chains. The geometry and rate of motions of the different groups in the side-chains were characterized below T_g by ^{2}H NMR spectroscopy.

Keywords: glass transition; α-relaxation; secondary relaxation; ^{2}H NMR; FID analysis; Field Cycling NMR relaxometry

1. Introduction

Amorphous polymers find numerous applications in the nonwovens, adhesives, textiles, printing and packaging, paints and coatings, construction, and paper industries. Macroscopic thermal, rheological and mechanical properties allowing these applications are strongly connected to structural and dynamic properties of the polymers at a molecular level [1]. In particular, on increasing the temperature, polymers undergo a hierarchy of motional processes that cover wide length and time scales, spanning from very fast localized fluctuations and conformational isomerizations, to segmental dynamics, to collective chain motions up to free translational diffusion of the whole chain [2].

The most dramatic change in polymer properties is observed at the glass transition. Different dynamic processes are important for glass formation in amorphous polymers, as highlighted by a variety of methods such as mechanical-dynamical spectroscopy, light spectroscopy, neutron scattering, broad band Dielectric Spectroscopy (DS), Nuclear Magnetic Resonance (NMR) spectroscopy, and specific heat spectroscopy. The most prominent process is the so-called α-relaxation, also referred to as structural (primary) relaxation or dynamic glass transition, due to segmental fluctuations related to conformational changes in the polymeric main-chain. In the melt state well above the glass transition temperature (T_g), the corresponding correlation time, τ_α, has typical values of about 10^{-13} s, describing localized segmental fluctuations, also referred to as "glassy dynamics"; with decreasing temperature, the correlation time increases very rapidly, reaching typical values of ~100 s at T_g. Most amorphous polymers show, in addition to the α-relaxation, secondary relaxations, named as β, γ, etc., due to local motions involving either pendant groups or main-chain units. A peculiar secondary relaxation, revealed by DS measurements on polymers without side-chains, is the Johari-Goldstein process, which has been considered as a generic feature of glass formation and can be regarded as a precursor for the glass transition [3]. On the other hand, in the case of polymers bearing side-chains, secondary relaxations associated to motions of the pendant groups were found [4–8]. Solid state NMR spectroscopy was revealed to be particularly useful in characterizing the mechanism of these motions [4,5].

Polyvinyl butyral (PVB) is an amorphous polymer widely used as an interlayer material in the manufacture of safety glass laminates, in solar photovoltaic modules, and as a binder in coatings, adhesives, enamels, and inks, thanks to its excellent optical clarity, adhesive properties, toughness, and flexibility [9–12]. The amorphous character of PVB arises from the random distribution of vinyl butyral and vinyl alcohol units, as well as from the presence of propyl side-chains on vinyl butyral units.

In spite of the large number of technological applications, only a few studies were reported concerning the dynamics of PVB [13–22]. Recently, PVB dynamics was investigated by some of us over broad frequency and temperature ranges by DS and ^{1}H field-cycling (FC) NMR relaxometry, focusing on a commercial sample [21]. DS allowed the α-relaxation to be characterized. Correlation times for this dynamic process (τ_α) were determined as a function of temperature, from which a dynamic glass transition temperature and a fragility index were extracted. Below T_g, a β-relaxation was found, and the corresponding correlation times (τ_β) were determined. ^{1}H FC NMR, a technique measuring the dependence (dispersion) of proton longitudinal relaxation rate (R_1) on the Larmor frequency (vide infra), was applied to study glassy dynamics above T_g up to T_g + 50 °C. The evolution of the R_1 dispersion curves with temperature indicated dynamic heterogeneity in proximity of the glass transition. Indeed, different dynamic properties can be envisaged for different segments of PVB considering that its structure includes a main-chain made of rigid units and quite long and more mobile alkyl side-chains (Figure 1).

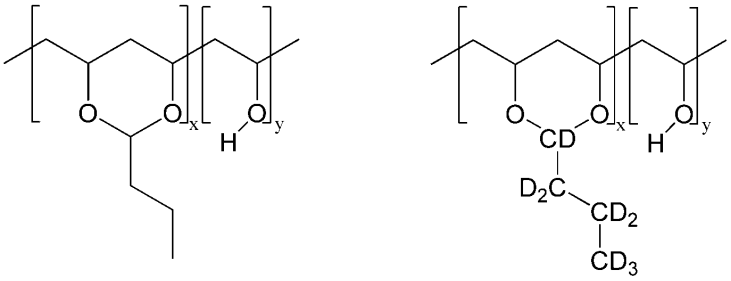

Figure 1. Structure of PVB-H and PVB-D. Fractions of vinyl butyral, x, and vinyl alcohol, y, are 0.6 and 0.4, respectively (see Supplementary Materials).

In order to better characterize the dynamics of PVB in the glassy and rubbery state and, in particular, to unravel the dynamics of side- and main-chains, in the present work

complementary NMR techniques were applied to two purposely synthesized PVB samples: PVB-H, fully protonated, and PVB-D, perdeuterated on the side-chains (Figure 1). In particular, the dynamics of the side-chains below T_g was investigated by ^{2}H NMR spectroscopy on PVB-D. The line shape of ^{2}H NMR spectra is determined by the modulation of the dominant quadrupolar interaction of ^{2}H nuclei by molecular motions, and information on the rate and mechanism of motion can be obtained from spectral line shape analysis [23,24]. In protonated moieties, the decay in time of the ^{1}H NMR signal (free induction decay, FID) is dominated by the effects of ^{1}H-^{1}H dipole-dipole couplings fluctuating because of molecular motions. Therefore, a strong connection exists between molecular mobility and ^{1}H time domain signals, with more mobile systems showing a more slowly decaying signal. Information on polymer dynamics can thus be obtained by FID analysis [25–27]. Here, FID's of PVB-H and PVB-D were analyzed at different temperatures to track the dynamics, mainly associated to the α-relaxation, across the glass transition. Finally, ^{1}H FC NMR relaxometry was applied to both PVB-H and PVB-D above T_g to more quantitatively characterize the dynamics of the different moieties. In fact, proton longitudinal relaxation results from the modulation of ^{1}H-^{1}H intra- and intermolecular dipolar interactions by polymer motions [28]. The possibility of measuring R_1 over a wide frequency range (0.01 to 40 MHz with commercial relaxometers) renders ^{1}H FC NMR relaxometry a powerful technique for investigating polymer dynamics. Here, experiments were performed up to 120 °C, corresponding to T_g + 55 °C. In the available frequency and temperature ranges, ^{1}H FC NMR relaxometry allowed glassy dynamics and propyl side-chain isomerizations to be investigated and correlation times to be estimated for these motions at the highest temperature. All together the applied techniques gave a picture of side- and main-chain motions over a quite broad temperature range, spanning from −223 °C to 120 °C, that is from T_g − 288 °C to T_g + 55 °C.

2. Materials and Methods

2.1. Materials

PVB-D was synthesized starting from polyvinyl alcohol (M_w = 31–50 kg/mol, 98–99% hydrolyzed) and butanal-d_8 according to Scheme 1 [29]. Butanal-d_8 was prepared oxidizing butanol-d_{10} with Dess-Martin periodinane, following Ref. [30]. The deuteration degree of PVB-D is >95%. PVB-H was synthesized adopting the same strategy but using polyvinyl alcohol (M_w = 31–50 kg/mol, 98–99% hydrolyzed) and butanal. Details of the synthetic procedures are reported in the Supporting Information. PVB-H and PVB-D were characterized by a molecular weight, M_w, of 101 and 106 kg/mol and a polydispersity of 1.6 and 2.0, respectively, as determined by size exclusion chromatography. T_g values, determined by DSC, were 65.6 °C for PVB-H and 64.0 °C for PVB-D. The molar fractions of vinyl butyral and vinyl alcohol units in PVB-H, determined according to Ref. [29] from ^{1}H NMR in $CDCl_3$, are 0.6 and 0.4, respectively.

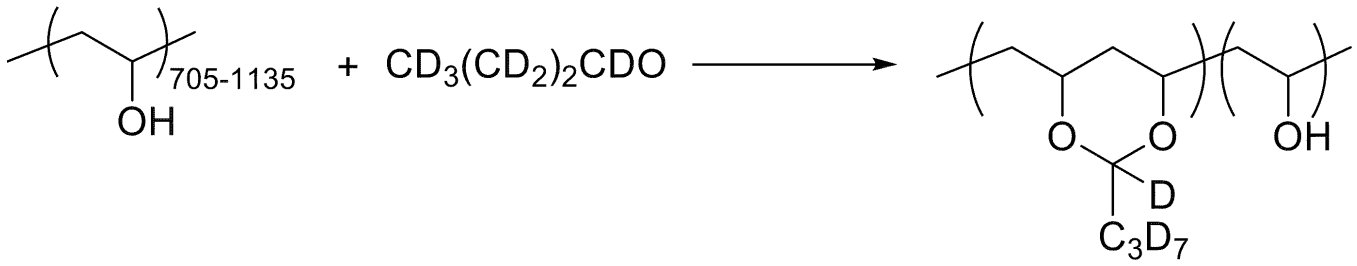

Scheme 1. Preparation of the deuterated polyvinyl butyral PVB-D.

2.2. Differential Scanning Calorimetry (DSC) and Size Exclusion Chromatography (SEC) Measurements

DSC experiments were performed using a Seiko SII ExtarDSC7020 calorimeter (Chiba, Japan) with the following thermal protocol: first cooling from 20 to 0 °C; at 0 °C for 2 min; first heating from 0 to 110 °C; 110 °C for 2 min; second cooling from 110 to 0 °C; at 0 °C for 2 min; second heating from 0 to 110 °C; at 110 °C for 2 min; third cooling from 110 to 20 °C. The cooling/heating rate was 10 °C/min in all runs, except for the third cooling, for which it was 30 °C/min. About 5 mg of polymer were used for each measurement. The T_g was determined using the tangents to the measured heat capacities below and above the heat capacity step via the Muse TA Rheo System software (version 3.0).

Molecular weight (M_w) and polydispersity were determined by SEC using an Agilent Technologies 1200 Series instrument equipped with two PLgel 5 mm MiniMIX-D columns (flux 0.3 mL/min) and a refraction index detector. Monodisperse poly(styrene) samples were used as calibration standards. The analysis was performed on a PVB solution in chloroform (2 mg/mL) filtered through a 0.2 mm filter prior to the measurement.

2.3. NMR Measurements

^{2}H NMR spectra were recorded at 46 MHz on a spectrometer constituted by a Magnex superconducting magnet and a Tecmag Apollo 500 NMR console and equipped with a probe mounted inside the Oxford Instruments CF1200 continuous flow cryostat. Measurements were performed between −223 and 20 °C. The temperature was regulated by the Oxford Instruments CT503 Temperature Controller to the accuracy of ± 0.1 °C. The quadrupole echo pulse sequence [31] was applied with appropriate phase cycling, with a 90° pulse duration of 5 μs and a time interval between the pulses of 50 μs. The spectra were obtained after Fourier Transformation of the signal collected from the echo maximum. The recycle delay ranged between 2 and 300 s depending on temperature. For the ^{2}H NMR measurements, the samples (200–300 mg) were enclosed in 5 mm o.d. glass tubes of 20 mm length that fitted the probe coil and sealed under vacuum.

Time domain ^{1}H NMR experiments were performed at a Larmor frequency of 20.7 MHz using a Niumag permanent magnet interfaced with a Stelar (Mede, Italy) PC-NMR console. Samples (100–200 mg) were enclosed in 5 mm o.d. NMR glass tubes, which were evacuated and flame sealed. ^{1}H FIDs were recorded on-resonance and in full-absorption mode receiver setting using both the direct excitation and the solid echo [32] pulse sequences with a 90° pulse duration of 3 μs and a recycle delay of 3 s and accumulating 128 transients. For the solid echo experiments, an echo delay of 14 μs was employed. Spectra were recorded at different temperatures between 30 and 100 °C. The temperature was controlled within ±0.2 °C by a Stelar VTC90 variable temperature controller and the sample was allowed to equilibrate for at least 10 min before measurement. The signal intensity was corrected according to the Curie law by multiplication with T/T_{ref}, with T_{ref} = 373 K. FID data up to 0.2 ms were considered in the analysis because the signal decay at longer times is affected by field inhomogeneities.

^{1}H longitudinal relaxation times (T_1) were measured at different Larmor frequencies using a Spinmaster FFC-2000 relaxometer (Stelar, Mede, Italy). The experiments were performed applying the prepolarizing and non-prepolarizing pulse sequences [33,34] below and above 10 MHz, respectively. The polarizing frequency was 25 MHz and the detection frequency 16.3 MHz. The 90° pulse duration was 10 μs and the switching time 3 ms. Four transients were accumulated and at least 16 values of the variable delay were used to build the magnetization trends. All the other parameters were optimized for each experiment. Samples (100–200 mg) were enclosed in 10 mm o.d. NMR glass tubes, which were evacuated and flame sealed. Measurements were performed at different temperatures in the 95 to 120 °C range, letting the sample temperature equilibrate for at least 10 min. The sample temperature was controlled within ± 0.2 °C by a Stelar VTC90 unit.

3. Results and Discussion

3.1. Dynamics of Side-Chains below T_g by ^{2}H NMR Spectroscopy

^{2}H NMR spectra were acquired on PVB-D at several temperatures between −223 °C and 20 °C to investigate the dynamics of the side-chains from the rigid limit up to T_g − 45 °C; a selection of spectra is shown in Figure 2. All the spectra result from the superposition of ^{2}H NMR subspectra relative to the different side-chain groups in PVB-D. In turn, each subspectrum is given by the sum of signals from all possible orientations of the C-D bonds in the amorphous sample (powder spectrum). In general, in a rigid powder spectrum one can observe inner singularities split by $2V_{yy} = \delta_0(1-\eta_0)$, inner edges separated by $2V_{xx} = \delta_0(1+\eta_0)$, and a total width of $2V_{zz} = 2\delta_0$. δ_0 and η_0 are the anisotropy and asymmetry parameters related to the ^{2}H electric field gradient tensor components and the quadrupolar coupling constant by the relationships

$$\delta_0 = \frac{3e^2qQ}{4\hbar} = \frac{3eQ}{4\hbar}V_{zz} \quad (1)$$

$$\eta_0 = \frac{V_{xx} - V_{yy}}{V_{zz}} \quad (2)$$

The asymmetry parameter η_0 is usually negligible in aliphatic C-D bonds. Therefore, when η_0 = 0, the inner singularities and edges converge, leading to strong singularities. This situation is observed at the lowest temperature for PVB-D (−223 °C, Figure 2), where a symmetric powder pattern is recorded, characterized by the typical quadrupolar splitting between inner singularities for aliphatic C-D bonds of 128 kHz (= $2V_{xx} = 2V_{yy} = \delta_0$) [35,36]. The spectral edges at ± 128 kHz corresponding to ± V_{zz} are smoothed due to finite pulse width [37].

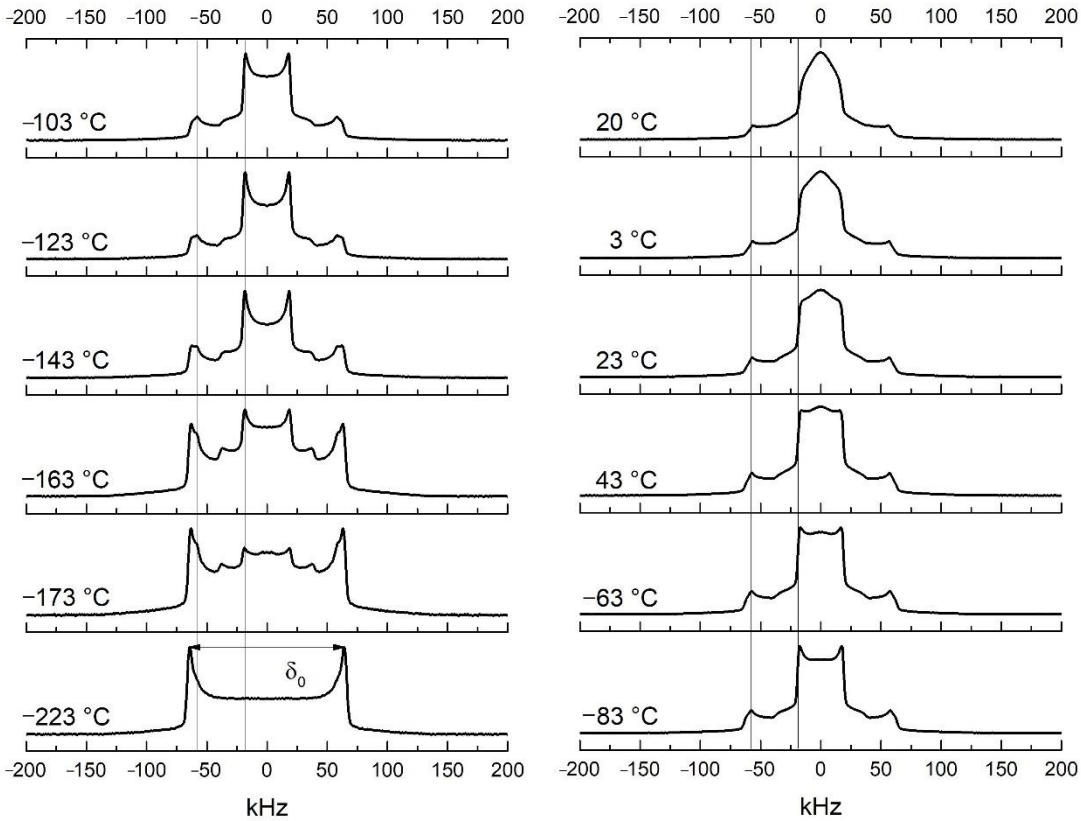

Figure 2. ^{2}H NMR spectra of PVB-D at the indicated temperatures. Vertical lines are guides for the eyes. The spectra were normalized to a constant height.

When C-D bonds undergo a rapid motion, characterized by a rate much greater than δ_0, an "averaged" spectrum results with singularities corresponding to averaged δ and η parameters, which depend on the motion geometry. For instance, for a methyl group rotating fast about its C3 axis, with deuterons subject to fast exchange between three equivalent sites of tetrahedral geometry, the singularities are expected to be split by $2V_{xx} = 2V_{yy} = \delta_0/3$ and $2V_{zz} = 2\delta_0/3$. If the motional rate is on the order of δ_0 (intermediate regime), the spectral line shape reflects both the rate and geometry of the motion. All this considered, the ^{2}H NMR spectrum at −173 °C can be interpreted as the superposition of a rigid component ascribable to methine (CD) and methylene (CD_2) groups and a narrower pattern, showing singularities at about ±18 kHz and ±37 kHz, due to the methyl group (CD_3). In particular, the shape of the latter component is compatible with that of a rotating methyl group in the intermediate regime. Indeed, the experimental spectral features are captured by a simulation including methyl deuterons undergoing three-site jumps with a rate of 4000 kHz and both rigid and mobile methine and methylene deuterons (Figure S4a). Indeed, the features observed at ±59 kHz (see vertical line at −59 kHz in Figure 2) indicate that at −173 °C, a fraction (~40%) of CD and CD_2 groups is not rigid anymore. At −123 °C, the rigid pattern has disappeared, and an averaged spectrum is observed for the CD and CD_2 groups characterized by singularities at ±58 kHz and inner edges at ±63 kHz (Figure 2), resulting in δ/δ_0 = 0.946 and η = 0.044. Similar line shapes were reported for deuterated methylene groups in the main-chain of poly(ethyl methacrylate) and poly(methyl methacrylate) [38] and of poly(ethylene-*alt*-propylene) [39] at temperatures below T_g and for methylene groups in the side-chains of poly(diethylsiloxane) in a crystalline phase [40]. This pattern can be interpreted as due to C-D bonds subject to a fast two-site jump motion in a cone, with cone angle of 70.5°, typical of tetrahedral symmetry, and flip angle of ~20° [40]. Upon heating, the pattern persists up to room temperature, but it slightly narrows and shows a progressively reduced asymmetry, as indicated by the values of δ/δ_0 and η extracted from the spectra and reported in Figure S5. The trends observed for these parameters cannot be rationalized by a simple increase of the flip angle, which would give a decrease of δ/δ_0 but an increase of η; instead, a motion more complicated than a two-site jump should be invoked, possibly involving a reorientation of the cone axis itself by a small flip angle. As a matter of fact, a fast motion characterized by small amplitudes is suggested by the modest narrowing of the pattern upon heating from −173 °C up to room temperature. As far as methyl is concerned, between −143 and −123 °C, the corresponding line shape shows the pattern expected for the fast rotation about the C3 axis (Figure 2), with a decreased signal intensity in the region between the ±18 kHz singularities. Indeed, at −123 °C, the ^{2}H NMR spectrum can be satisfactorily reproduced by a combination of two subspectra, one due to CD_3 groups rotating fast about their ternary axes and the other arising from CD and CD_2 moieties undergoing fast two-site jumps (Figure S4b). Upon heating up to room temperature, the methyl signal intensity increases in the central part of the spectrum, and there is a partial collapse of the singularities at ±18 kHz (Figure 2); these features are indicative of the onset of a motion of the methyl axis further averaging the residual quadrupolar interaction [41–43]. All in all, at 20 °C (=T_g − 45 °C), the highest temperature we could set in our instrument, the side-chains are still subjected to small amplitude motions. At this temperature, the CD_2 and CD groups experience a fast spatially restricted motion, whereas the methyl group undergoes both a fast motion about its C3 axis and a slower motion involving the C3 axis itself. This motion is not isotropic yet and occurs at rates on the order of the residual quadrupolar interaction.

Further information on the dynamics of the PVB side-chains arises from the total intensity of the ^{2}H NMR spectra as a function of temperature, as well as from the relative intensity of the spectral contributions due to the different groups. Indeed, distortions in the line shape and significant loss of signal intensity can be observed in ^{2}H NMR spectra acquired with the quadrupolar echo pulse sequence when motions of the C-D bonds occur in the so-called intermediate regime, i.e., when the motional rates are of the order of δ_0 [31], while insignificant and little intensity loss is expected for motions in the slow and

fast regime, respectively [41–45]. Moreover, spectral distortions and signal loss depend on the echo delay and on the motion geometry. In particular, it has been shown that spatially restricted motions with correlation times on the order of the quadrupolar echo time, as in the case for secondary relaxation processes in glasses, lead to strong loss of the spectral intensity for echo times longer than few tens μs [46–48].

The total integrated signal intensity of the ^{2}H spectra recorded on PVB-D at various temperatures reported in Figure 3 shows a rapid and pronounced decrease from −223 to −173 °C, while at higher temperatures a less steep decrease is observed. The signal loss is associated to the presence of motions in the intermediate regime. Therefore, in the recorded spectra, the contributions of groups undergoing slow and fast motions are enhanced, although a distribution of motional rates is probably present. At −173 °C, the spectral contributions from CD_3 moieties (0.37) and from CD_2 and CD groups (0.63), as reported in Figure S4a, are close to the value expected on the basis of the chemical structure of the side chain (0.30 and 0.70, respectively). Therefore, motions in the intermediate regime affect all the propyl chain groups. At higher temperatures, by looking at the evolution of the relative intensities of the outer and inner parts of the spectra in Figure 2, mainly ascribed to CD and CD_2 groups and to CD_3 groups, respectively, a collapse is observed for the intensity of the outer part with respect to that of the inner part at −143 °C. Then the relative intensity of the outer part of the spectra only slightly decreases by further increasing the temperature up to 20 °C. The simulation of the line shape at −123 °C indicates a spectral contribution from CD_2 and CD of only 0.24, paralleled by a CD_3 contribution of 0.76. Similarly, a selective signal loss of methine and methylene groups with respect to methyl groups was observed below T_g in poly(ethylene-*alt*-propylene) [39]. This feature was ascribed to the different behavior of C-D bonds in methine and methylene groups undergoing restricted angular displacements (i.e., wobbling in a cone with an angle of 11°–31°, depending on the temperature) in contrast to that of methyl groups, which also show fast rotation about their C3 axis. In our case, the reorientation in a cone for the CD_2 and CD groups, with a flip angle of ∽20°, results in a significant loss of their signal compared to that of CD_3.

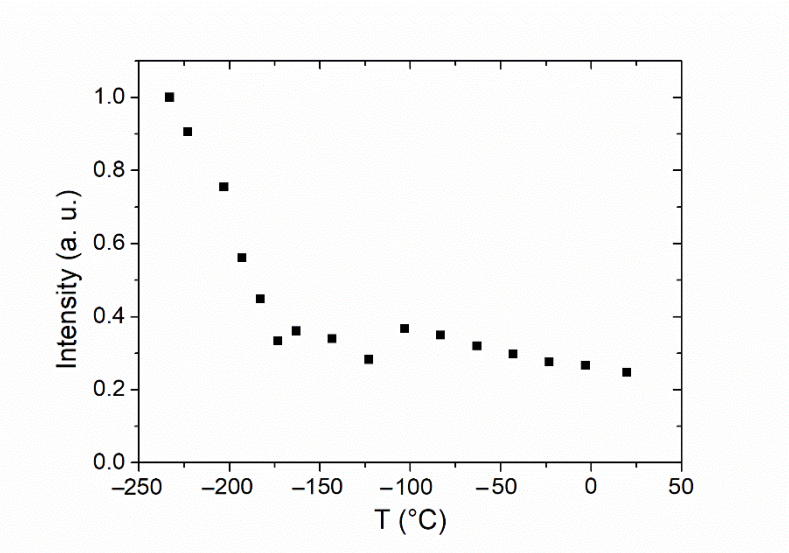

Figure 3. Integral signal intensity of ^{2}H NMR spectra of PVB-D collected with a solid echo delay of 50 μs at various temperatures. The intensities were divided by the intensity of the spectrum at −223 °C.

3.2. Dynamics of Main- and Side-Chains across T_g from ^{1}H FID Analysis

In order to gain information on the dynamics of main- and side-chain segments across T_g, the ^{1}H FIDs of PVB-H and PVB-D were acquired between 30 and 100 °C, corresponding to temperatures of T_g − 35 °C and T_g + 35 °C, using both the solid echo and the direct excitation pulse sequences; data collected using these sequences are shown in Figures 4, 5 and S6. The observed signals arise from both main- and side-chain hydrogens for PVB-H, but from the sole main-chain hydrogens for PVB-D. The polymer mobility can be investigated by studying the FID signal, a fast decay of the signal corresponding to the response of the rigid glassy polymer segments and a slower one to that of mobile segments. However, the FID acquired by direct excitation (i.e., the decays of the transverse magnetization after a 90° pulse) cannot be directly exploited to obtain the signal arising from polymer segments in the glassy state showing significant decay within 20 μs. In fact, the first 14 μs of the FID, containing the initial fast decaying part of the signal, are missing because of the dead time of the spectrometer receiver. An accurate measurement of the shape of the initial part of the FID for a rigid phase can instead be obtained with the solid echo pulse sequence because it avoids the dead time of the spectrometer. However, the amplitude of the echo signal can be lower than its true value because the solid echo does not fully refocus the multi-spin dipolar interactions present in a proton dipolar network. Moreover, further signal loss may occur for polymer segments undergoing motions with correlation times comparable to the echo time. All this considered, in our analysis we adopted the following strategy: (i) the solid echo FIDs were used to obtain information on the shape of the signal decay for PVB-H and PVB-D, and therefore on the polymer dynamics; (ii) the FIDs recorded by direct excitation were exploited to quantitatively determine the signal intensity arising from all protons in the polymers [49,50]; (iii) the comparison of the echo amplitude at maximum with the reconstructed intensity at t = 0 of the direct excitation FID was employed for quantifying the signal losses due to polymer dynamics on a time scale on the order of the echo delay (10–100 μs).

In the glassy state at 30 °C, for both PVB isotopomers, most of the signal decays were within 25 μs (Figure 4), indicating that almost all the hydrogens are in rigid environments with characteristic motion frequencies smaller than tens of kHz on the order of the static ^{1}H-^{1}H dipolar couplings. The remaining hydrogens contribute to a more slowly decaying FID component, which is larger for PVB-H than for PVB-D. In the case of PVB-D, the fast-decaying part of the FID shows a "hole" at about 30 μs, typical of a Pake profile, arising from the dominant dipolar coupling between ^{1}H nuclei in CH_2 groups in the vinyl butyral and vinyl alcohol units. For PVB-H, the Pake "hole" is smeared out, most probably because of the presence of a larger number of ^{1}H-^{1}H pairs with different dipolar couplings. For both PVB-D and PVB-H, the FIDs at 30 °C were fitted to the sum of an Abragamian function and an exponential function:

$$I(t) = w_{Abr}\frac{sin(2\pi\nu t)}{2\pi\nu t}e^{-(t/T_{2,Abr})^2} + w_{exp}e^{-(t/T_{2,exp})} \quad (3)$$

The Abragamian function is a Gaussian broadened *sinc* function introduced by Abragam [51], which is generally used to reproduce the signal decay associated to a Pake spectrum. In Equation (3), w_i, with $i = Abr, exp$, represents the weight fraction of hydrogen nuclei in domain i and $T_{2,i}$ the corresponding time constant. A good reproduction of the FIDs (see Figure 4) was obtained with ν = 19922 s^{-1} for both isotopomers and with $T_{2,Abr}$ = 26 μs, w_{exp}= 0.28 and $T_{2,\mathrm{exp}}$ = 22 μs for PVB-H and $T_{2,Abr}$ = 22 μs, w_{exp}= 0.11 and $T_{2,\mathrm{exp}}$ = 30 μs for PVB-D. The small T_2 values associated to both components indicate that slow and/or amplitude restricted dynamics occur in both PVB-D and PVB-H at T_g − 35 °C. Second moment values, M_2, of 6.7·10^9 and 7.3·10^9 rad^2 s^{-2} are associated to the main Abragamian component for PVB-H and PVB-D, respectively.

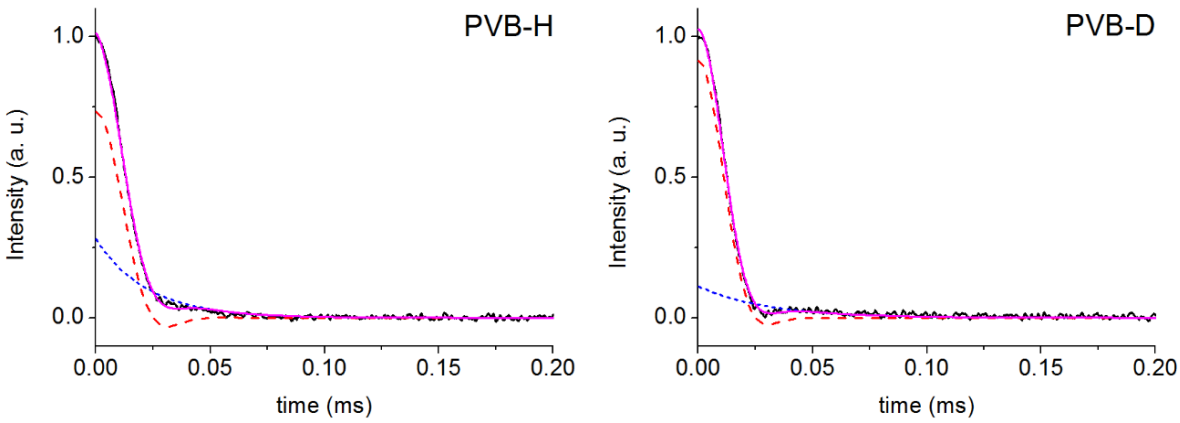

Figure 4. Analysis of the ^{1}H FIDs (black full lines), recorded by the solid echo pulse sequence on PVB-H (**left**) and PVB-D (**right**) at 30 °C, as a sum (purple full lines) of an Abragamian function (red dashed lines) and an exponential function (blue short-dashed lines).

Upon increasing the temperature up to T_g + 35 °C, the evolution of the signal reflects the motional narrowing phenomenon associated to the glass-rubber transition (Figures 5 and S6). A comparison between FIDs acquired at the same temperature for the two isotopomers shows a slower signal decay for PVB-H with respect to PVB-D at all the temperatures, indicating faster dynamics. In order to extract semi-quantitative information, we used the Anderson–Weiss (A-W) model [52] to analytically express the FID of a dipolarly coupled spin pair subject to isotropic rotational diffusion:

$$\mathrm{I}(t) \approx exp\left[-M_2\tau_c^2\left(e^{-t/\tau_c}+\frac{t}{\tau_c}-1\right)\right] \quad (4)$$

where the second moment, M_2, is approximately equal to $(9/20)D_{HH}^2$, with D_{HH} representing the largest dipole–dipole pair coupling. τ_c indicates the correlation time associated to rotational diffusion. Here, τ_c represents the correlation time for the main-chain segmental reorientations (α-process) for PVB-D, whereas it non-trivially results from a combination of main-chain and faster side-chain motions for PVB-H. The A-W model was previously applied to analyze the FID signals of poly(ethyl acrylate) around and in particular above T_g [49]. This model satisfactorily fits the experimental signal decays of PVB-H and PVB-D, obtained by both solid echo (Figure 5) and direct excitation (Figure S6) pulse sequences, with M_2 taken from the fit to the Abragamian function and τ_c values as reported in the figures. Between 70 and 100 °C, τ_c decreases from tens of microseconds to approximately one microsecond, with small differences between values extracted from signals acquired by the two techniques. PVB-D shows longer τ_c values compared to PVB-H at the same temperature. Therefore, main-chain segmental fluctuations associated to the α-process, selectively detected in PVB-D, are slower than the combined dynamic process revealed in PVB-H, where faster side-chain motions affect the observed τ_c.

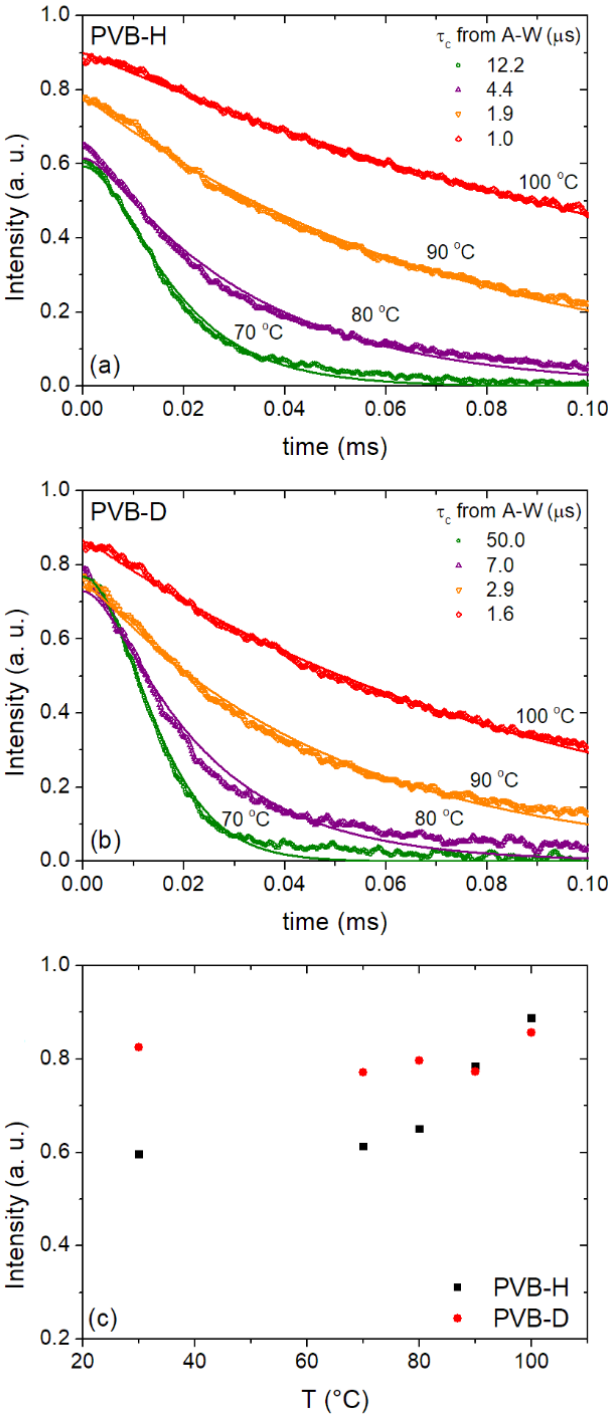

Figure 5. ^{1}H FIDs recorded on PVB-H (**a**) and PVB-D (**b**) at the indicated temperatures with the solid echo pulse sequence (symbols) and fitting curves to Equation (4) (solid lines). (**c**) Intensity of the signal at the top of the echo divided by the intensity of the FID at $t = 0$ recorded by direct excitation at the reference temperature (100 °C). FID intensities were corrected according to the Curie law.

Further information on the dynamic behavior of PVB-D and PVB-H was obtained by quantifying the signal losses in solid echo experiments. To this aim, the signal intensities at the top of the solid echoes were corrected according to the Curie law and divided by the value at $t = 0$ of the direct excitation signal at the reference temperature (100 °C). In turn, the latter intensity was obtained from the fit of the signal to the A-W equation. The

obtained results are shown in Figure 5c. Both samples exhibit signal losses at all the investigated temperatures. These losses are due to both unrefocused multi-spin ^{1}H-^{1}H dipolar interactions by the solid echo pulse sequence and molecular motions taking place during the echo delay in the intermediate regime, i.e., on the time scale of the refocused dipolar interaction (10–100 kHz). The larger signal loss observed for PVB-H with respect to PVB-D up to 80 °C can be ascribed to the larger number of multi-spin interactions present in PVB-H due to the larger amount of neighboring protons in this isotopomer. Starting from 80 °C, a faster recovery of the signal intensity is observed for PVB-H, most probably because many segments are undergoing fast motions with correlation times much shorter than 10 μs, especially in the side-chains.

3.3. Dynamics of Main- and Side-Chains above T_g from ^{1}H FC NMR Relaxometry

^{1}H longitudinal relaxation rates ($R_1 = 1/T_1$) were measured as a function of Larmor frequency between 0.3 and 35 MHz on both PVB-H and PVB-D at several temperatures above T_g (95–120 °C) in order to get insight into the dynamics of the main- and side-chains over a broad frequency range. At all frequencies and temperatures, a single R_1 value was measured, indicating that spin diffusion is effective. R_1 values could not be measured at lower frequencies because of limitations due to the relaxometer switching time. As shown in Figure 6, for PVB-D R_1 values increase by increasing the temperature, indicating that for temperatures up to T_g + 55 °C motions of the main-chain segments are in the slow regime. Considering the frequency range observed, we can infer that dynamics occurs with a correlation time $\tau > 5 \cdot 10^{-7}$ s at 120 °C. On the other hand, an increasing trend of R_1 with temperature is observed for PVB-H at frequencies above 1 MHz, while R_1 reaches a maximum and then decreases at lower frequencies for $T > 105$ °C. This behavior is exemplified in Figure 7a, where the trend of R_1 as a function of the inverse temperature is shown at the Larmor frequency of 0.5 MHz. A maximum of R_1 is found at 110 °C, indicating that the motional frequency matches the measuring frequency. An estimate of the correlation time for the motion governing relaxation in the observed frequency range can be obtained by the relationship at the maximum of R_1, $\omega\tau \cong 1$; a value of τ of ~$3 \cdot 10^{-7}$ s is determined. This value is in agreement with that previously determined for commercial PVB at the same temperature [21].

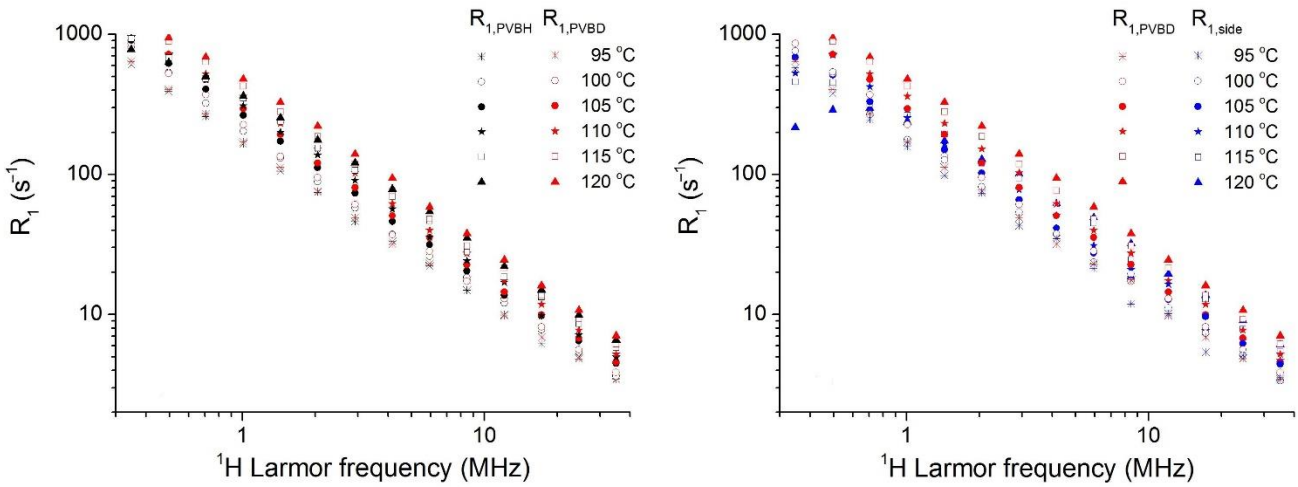

Figure 6. ^{1}H R_1 of PVB-H (black symbols) and PVB-D (red symbols) and $R_{1,side}$ (blue symbols) as a function of Larmor frequency at the indicated temperatures. $R_{1,side}$ values were obtained using Equation (5).

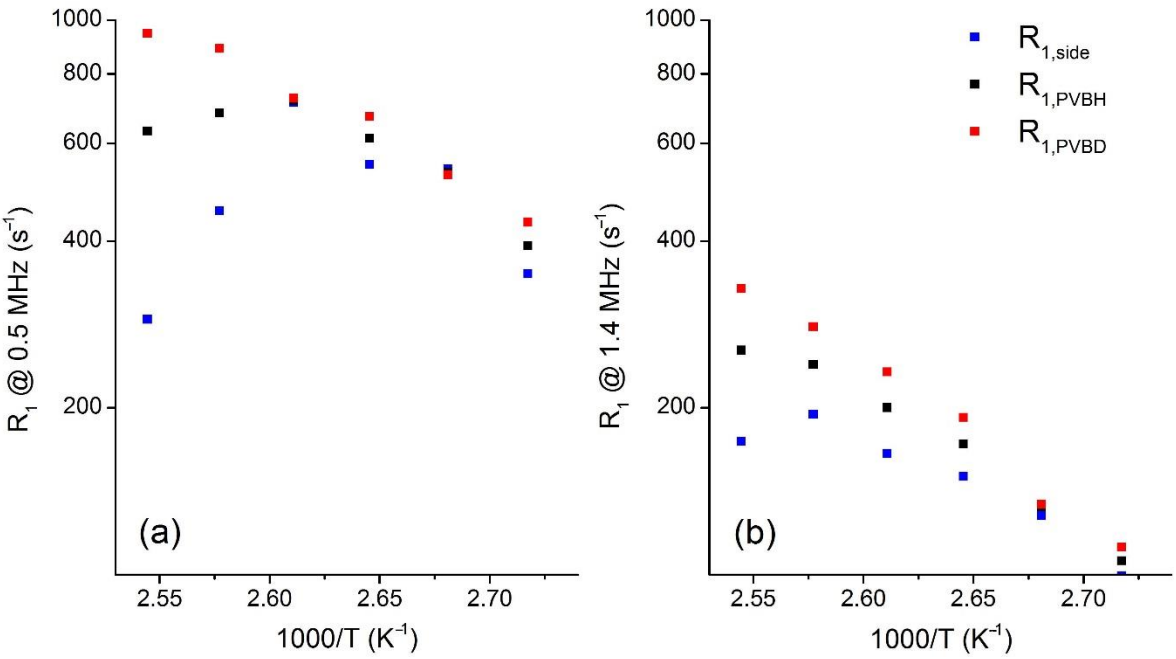

Figure 7. (**a**) ^{1}H R_1 of PVB-H and PVB-D and $R_{1,side}$ at 0.5 MHz as a function of inverse temperature. (**b**) ^{1}H R_1 of PVB-H and PVB-D and $R_{1,side}$ at 1.4 MHz as a function of inverse temperature.

If R_1 data recorded at the same temperature on the two isotopomers are compared, lower values are observed at each frequency for PVB-H with respect to PVB-D. This feature is surprising if we consider the higher number of proton dipolar couplings contributing to relaxation in PVB-H with respect to PVB-D. In fact, in a polymer, each proton relaxes with a rate given by the sum of the dipolar interactions with all the other protons (interactions with deuterons in the case of PVB-D are negligible), weighted by r^{-6}, r being the distance between proton pairs [53,54]. As a consequence, the relaxation strength should decrease in the deuterated sample, as previously observed for selectively deuterated polyisoprene [55]. The observed feature can instead be accounted for by considering that, due to spin diffusion, in PVB-H R_1 represents an average over both side- and main-chain protons, whereas in PVB-D, only the main-chain protons contribute to relaxation. Assuming that PVB-D and PVB-H have the same fractions of vinyl butyral and vinyl alcohol units and that the main-chain dynamics does not change at a given temperature for the two isotopomers (M_w and T_g are quite similar), we can express the relaxation rate of PVB-H, $R_{1,PVBH}$, as the average of the relaxation rate of PVB-D, $R_{1,PVBD}$, due to main-chain protons, and that for the side-chain protons, $R_{1,side}$, weighted by the molar fractions of hydrogens in the main- (f_{main} = 0.52) and side- (f_{side} = 0.48) chains arising from the stoichiometric composition of PVB-H:

$$R_{1,PVBH} = f_{main}R_{1,PVBD} + f_{side}R_{1,side} \quad (5)$$

Another assumption of this approach is that, based on distance considerations, the observed R_1 values are dominated by the fluctuations of dipolar interactions between two protons bound to the same carbon atoms and thus both belonging either to the main-chain or to a side-chain, while only minor contributions arise from dipolar interactions between a proton located on a side-chain and one located on the main-chain. Using Equation (5), $R_{1,side}$ was determined at each temperature and frequency starting from the experimental relaxation rates. The obtained $R_{1,side}$ values, shown in Figure 6, are always smaller than the corresponding $R_{1,PVBD}$ values, the difference between them increasing with decreasing the frequency and increasing the temperature. At 120 °C, $R_{1,side}$ shows a plateau below 1 MHz, indicating that side-chain dynamics has entered the motional narrowing regime. Looking

at the relaxation rates as a function of temperature, maxima are observed for $R_{1,side}$ at frequencies ≤1.4 MHz. In particular, at 0.5 MHz, the $R_{1,side}$ maximum occurs at ~110 °C as for PVB-H (Figure 7b). Therefore, the maximum detected for PVB-H can be ascribed to the side-chain motion. At 1.4 MHz, the $R_{1,side}$ maximum is found at ~115 °C (Figure 7a); correspondingly, a value of ~$1.1 \cdot 10^{-7}$ s is determined for the correlation time of the side-chain motion.

The interpretation of the FC NMR data confirms the results of the ^{1}H FID analysis concerning the faster dynamics of the side-chains compared to the main-chain. It also provides an estimate for the correlation time of the side-chain motion, i.e., ~$1.1 \cdot 10^{-7}$ s at 115 °C. Moreover, a lower boundary of $5 \cdot 10^{-7}$ s can be set for the correlation time of the main-chain at 120 °C, the highest investigated temperature. These values are in line with those estimated by the Anderson–Weiss analysis of the ^{1}H FIDs up to 100 °C.

If we compare these results with our previous findings on commercial PVB [21], we can state that the estimated value for the correlation time of the main-chain motion agrees with that determined for the α-relaxation by DS measurements. On the other hand, the correlation time of the side-chain motion at 115 °C is much longer than that associated to the β-relaxation as extrapolated at the same temperature from DS data. As a matter of fact, the dynamics of the propyl side-chains, associated to a very small variation of the electric dipole, is likely not to significantly affect dielectric relaxation.

4. Conclusions

Three NMR spectroscopy and relaxometry methods were applied to investigate the dynamics of the propyl side-chains and of the main-chain of PVB over a wide temperature range, spanning from −223 to 120 °C (i.e., from T_g − 288 °C to T_g + 55 °C), exploiting the PVB-D and PVB-H isotopomers. For the side-chains at temperatures lower than T_g, ^{2}H NMR experiments revealed heterogeneous dynamics for all the groups, with a significant amount of groups undergoing motions in the intermediate regime (10^4–10^6 Hz), leading to significant signal losses starting from −173 °C. The analysis of the line shapes of ^{2}H NMR spectra indicates that the methine, methylene, and methyl groups undergo motions characterized by frequencies smaller than 10^5 Hz up to –173 °C. At this temperature, the methyl groups are subjected to a three-site jump motion around the C3 axis with a rate of $4 \cdot 10^6$ Hz, while a small fraction of CD and CD_2 groups undergo a two-site jump motion in a cone with a flip angle of ∽20°. Upon heating, the methyl motion speeds up and an additional reorientation of the C3 axis occurs. At the same time, the motion of the CD and CD_2 groups becomes faster and a reorientation of the cone axis itself likely shows up. At 20 °C, corresponding to T_g − 45 °C, the motions of all the moieties are still highly spatially restricted.

^{1}H FID analysis corroborates this picture, showing that at T_g − 35 °C, the dynamics of both PVB-D and PVB-H is quite far from the motional narrowing, since motions of the main-chain are slow and motions of side-chains, although faster, are quite restricted in amplitude. On increasing the temperature, a progressively faster and more isotropic dynamics is observed above T_g. At the highest achieved temperature (T_g + 35 °C) a correlation time of 1.6 μs is estimated for the α-relaxation in PVB-D, while a shorter effective correlation time (1.0 μs), also accounting for the faster motions in the side-chains, results for PVB-H.

The different dynamics of main-chain and propyl side-chains is further highlighted by ^{1}H FC NMR. Indeed, while the main-chain undergoes conformational reorientations associated to the α-relaxation, as detected in previous DS measurements, the side-chain moieties experience a faster secondary motion, here revealed for the first time and likely undetectable by DS. At 115 °C, the side-chains' motion is at least 5 times faster than that of the main-chain. The β-relaxation reported in the DS investigations is outside the frequency range here investigated.

From a methodological point of view, we can state that the combination of NMR techniques and selective isotopic labeling here employed were revealed to be particularly

useful for unravelling both the rate and mechanism of main- and side-chain motions in PVB. Measurements at higher temperatures are envisaged with all NMR methods in order to extend this study and further explore the motions of main- and side-chains over a broader frequency range.

Supplementary Materials: The following are available online at www.mdpi.com/article/10.3390/polym13162686/s1. Figure S1. 13C NMR spectrum of butanal-d8 in CDCl3. Figure S2. 1H NMR spectra of PVB-D (bottom) and PVB-H (top) in CDCl3. Figure S3. 13C NMR spectra of PVB-D (bottom) and PVB-H (top). Figure S4. (a) Comparison between the experimental 2H NMR spectrum of PVB-D at -173 °C (black line) and a simulated spectrum (red line) resulting from the superposition of: a rigid spectrum (42%); the spectrum of methylene and methine deuterons undergoing fast two site jumps in a cone with an angle of 20° (28%); the spectrum of methyl deuterons subject to a three-site jump motion with a rate of 4000 kHz (30%). (b) Comparison between the experimental 2H NMR spectrum of PVB-D at -123 °C (black line) and a simulated spectrum (red line) resulting from the superposition of: the spectrum of methylene and methine deuterons undergoing fast two site jumps in a cone with an angle of 20° (24%); the spectrum of methyl deuterons subject to a fast three-site jump motion (76%). The simulations were carried out using NMR Weblab. Figure S5. Normalized anisotropy (red circles) and asymmetry parameter (black squares) derived from the methane and methylene pattern in the experimental 2H NMR spectra of PVB-D at the indicated temperatures. Figure S6. 1H FIDs recorded on PVB-H (left) and PVB-D (right) at the indicated temperatures (symbols) by direct excitation and fitting curves (solid lines) to Anderson-Weiss (Eq. 4). Signal intensities were corrected according to the Curie law using the highest temperature as reference. The best fit correlation times (τc) are also reported.

Author Contributions: Conceptualization, S.P. and L.C.; Methodology, A.M., S.P. and L.C.; Validation, S.P. and L.C.; Formal Analysis, S.P. and L.C.; Investigation, S.P., L.C., C.D.M., L.R., A.B., Z.T.L., S.B. and A.M.; Data Curation, S.P., S.B., A.M. and A.B.; Writing—Original Draft Preparation, L.C., S.P., A.M.; Writing—Review and Editing, L.C., A.M., A.B., Z.T.L. and S.P.; Project Administration, S.P. and L.C.; Funding Acquisition: S.B. and S.P. All authors have read and agreed to the published version of the manuscript.

Funding: This work was partially supported by Regione Toscana in the framework of the project SELFIE (Bando FAR-FAS 2014- Programma PAR FAS 2007-2013-Linea d'Azione 1.1) and by Fondazione Cassa di Risparmio di Pisa (PREVISION Project- Avviso 2016 per il Settore della Ricerca Scientifica e Tecnologica).

Data Availability Statement: The data presented in this study are available on request from the corresponding author.

Acknowledgments: We acknowledge the contribution of the COST Action 15209 (Eurelax: European Network on NMR Relaxometry) and of the Italy-Poland CNR/PAS 2020-2021 bilateral project "Multidisciplinary studies of structural and dynamic properties of glass forming compounds". The authors would like to thank Marco Geppi (Università di Pisa) for letting them use the 20.7 MHz spectrometer.

Conflicts of Interest: The authors declare no conflict of interest.

References

1. Schönhals, A.; Kremer, F. Amorphous Polymers. In *Polymer Science: A Comprehensive Reference*; Matyjaszewski, K., Möller, M., Eds.; Elsevier BV: Amsterdam, The Netherlands, 2012; Volume 1, pp. 201–226.
2. Kimmich, R.; Fatkullin, N. Polymer Chain Dynamics and NMR. *Adv. Polym. Sci.* **2004**, *170*, 1–113.
3. Johari, G.P.; Goldstein, M. Viscous Liquids and the Glass Transition. II. Secondary Relaxations in Glasses of Rigid Molecules. *J. Chem. Phys*. **1970**, *53*, 2372–2388.
4. Schmidt-Rohr, K.; Kulik, A.S.; Beckham, H.W.; Ohlemacher, A.; Pawelzik, U.; Boeffel, C.; Spiess, H.W. Molecular Nature of the β Relaxation in Poly(methyl methacrylate) Investigated by Multidimensional NMR. *Macromolecules* **1994**, *27*, 4733–4745.
5. Kulik, A.S.; Beckham, H.W.; Schmidt-Rohr, K.; Radloff, D.; Pawelzik, U.; Boeffel, C.; Spiess, H.W. Coupling of the α and β Processes in Poly(ethyl methacrylate) Investigated by Multidimensional NMR. *Macromolecules* **1994**, *27*, 4746–4754.
6. Genix, A.-C.; Lauprêtre, F. Subglass and Glass Transitions of Poly(di-*n*-alkylitaconate)s with Various Side-Chain Lengths: Dielectric Relaxation Investigation. *Macromolecules* **2005**, *38*, 2786–2794.
7. Gaborieau, M.; Graf, R.; Kahle, S.; Pakula, T.; Spiess, H.W. Chain Dynamics in Poly(*n*-alkyl acrylates) by Solid-State NMR, Dielectric, and Mechanical Spectroscopies. *Macromolecules* **2007**, *40*, 6249–6256.

8. Mpoukouvalas, K.; Floudas, G.; Williams, G. Origin of the α, β, (βα), and "Slow" Dielectric Processes in Poly(ethyl methacrylate). *Macromolecules* **2009**, *42*, 4690–4700.
9. Liau, L.C.K.; Viswanath, D.S. Thermal Degradation of Poly(vinylbutyral)/Ceramic Composites: A Kinetic Approach. *Ind. Eng. Chem. Res*. **1998**, *37*, 49–57.
10. Boddu, V.M.; Viswanath, D.S.; Natarajan, G.; Knickerbocker, J.V. Activity and Reactivity of Carbon Formed by the Thermal Degradation of Poly(vinylbutyral) in Alumina Pellets. *J. Am. Ceram. Soc*. **1990**, *73*, 1620–1625.
11. Carrot, C.; Bendaoud, A.; Pillon, C. *Handbook of Thermoplastics*, 2nd ed.; Olabis, O., Adewale, K., Eds.; Taylor & Francis Group: Abingdon, UK; CRC Press: Boca Raton, FL, USA, 2016; Chapter 3.
12. Martín, M.; Centelles, X.; Solé, A.; Barreneche, C.; Fernández, I.; Cabeza, L.F. Polymeric Interlayer Materials for Laminated Glass: A Review. *Constr. Build. Mater*. **2020**, *230*, 116897.
13. Hooper, P.A.; Blackman, B.R.K.; Dear, J.P. The Mechanical Behaviour of Poly(vinyl butyral) at Different Strain Magnitudes and Strain Rates. *J. Mater. Sci.* **2012**, *47*, 3564–3576.
14. Andreozzi, L.; Briccoli Bati, S.; Fagone, M.; Ranocchiai, G.; Zulli, F. Dynamic Torsion Tests to Characterize the Thermo-viscoelastic Properties of Polymeric Interlayers for Laminated Glass. *Constr. Build. Mater*. **2014**, *65*, 1–13.
15. Arayachukiat, S.; Siriprumpoonthum, M.; Nobukawa, S.; Yamaguchi, M. Viscoelastic Properties and Extrusion Processability of Poly(vinyl butyral). *J. Appl. Polym. Sci*. **2014**, *131*, 40337–40344.
16. Takahashi, Y. Dielectric α- and β-Dispersions in Polyvinyl Butyral (PVB). *J. Phys. Soc. Jpn.* **1961**, *16*, 1024.
17. Funt, B.L. Dielectric Dispersion in Solid Polyvinyl Butyral. *Can. J. Chem*. **1952**, *30*, 84–91.
18. Mehendru, P.C.; Kumar, N.; Arora, V.P.; Gupta, N.P. Dielectric Relaxation Studies in Polyvinyl butyral. *J. Chem. Phys*. **1982**, *77*, 4232–4235.
19. Saad, G.R.; El-Shafee, E.; Sabaa, M.W. Dielectric and Mechanical Properties in the Photodegradation of Poly(vinyl butyral) Films. *Polym. Degrad. Stab*. **1995**, *47*, 209–215.
20. Handge, U.A.; Wolff, M.F.H.; Abetz, V.; Heinrich, S. Viscoelastic and Dielectric Properties of Composites of Poly(vinyl butyral) and Alumina Particles with a High Filling Degree. *Polymer* **2016**, *82*, 337–348.
21. Pizzanelli, S.; Prevosto, D.; Labardi, M.; Guazzini, T.; Bronco, S.; Forte, C.; Calucci, L. Dynamics of Poly(vinyl butyral) Studied Using Dielectric Spectroscopy and ^{1}H NMR Relaxometry. *Phys. Chem. Chem. Phys*. **2017**, *19*, 31804–31812.
22. Pizzanelli, S.; Forte, C.; Bronco, S.; Guazzini, T.; Serraglini, C.; Calucci, L. PVB/ATO Nanocomposites for Glass Coating Applications: Effects of Nanoparticles on the PVB Matrix. *Coatings* **2019**, *9*, 247.
23. Schmidt-Rohr, K.; Spiess, H.W. *Multidimensional Solid-State NMR and Polymers*; Academic Press: London, UK, 1994.
24. Macho, V.; Brombacher, L.; Spiess, H.W. The NMR-WEBLAB: An Internet Approach to NMR Lineshape Analysis. *Appl. Magn. Reson*. **2001**, *20*, 405–432.
25. Schäler, K.; Roos, M.; Micke, P.; Golitsyn, Y.; Seidlitz, A.; Thurn-Albrecht, T.; Schneider, H.; Hempel, G.; Saalwächter, K. Basic Principles of Static Proton Low-Resolution Spin Diffusion NMR in Nanophase-Separated Materials with Mobility Contrast. *Solid State Nucl. Magn. Reson*. **2015**, *72*, 50–63.
26. Hansen, E.W.; Kristiansen, P.E.; Pedersen, B. Crystallinity of Polyethylene Derived from Solid-State Proton NMR Free Induction Decay. *J. Phys. Chem. B* **1998**, *102*, 5444–5450.
27. Borsacchi, S.; Sudhakaran, U.P.; Calucci, L.; Martini, F.; Carignani, E.; Messori, M.; Geppi, M. Rubber-Filler Interactions in Polyisoprene Filled with In Situ Generated Silica: A Solid State NMR Study. *Polymers* **2018**, *10*, 822.
28. Kimmich, R. *Field-Cycling NMR Relaxometry: Instrumentation, Model Theories and Applications*; Royal Society of Chemistry: London, UK, 2019.
29. Fernández, M.D.; Fernández, M.J.; Hoces, P. Synthesis of Poly(vinyl butyral)s in Homogeneous Phase and Their Thermal Properties. *J. Appl. Polym. Sci*. **2006**, *102*, 5007–5017.
30. Dess, D.B.; Martin, J.C. A Useful 12-I-5 Triacetoxyperiodinane (The Dess-Martin Periodinane) for the Selective Oxidation of Primary or Secondary Alcohols and a Variety of Related 12-I-5 Species. *J. Am. Chem. Soc*. **1991**, *113*, 7277–7287.
31. Vega, A.J.; Luz, Z. Quadrupole Echo Distortion as a Tool for Dynamic NMR: Application to Molecular Reorientation in Solid Trimethylamine. *J. Chem. Phys*. **1987**, *86*, 1803– 1813.
32. Powles, J.G.; Strange, J.H. Zero Time Resolution Nuclear Magnetic Resonance Transient in Solids. *Proc. Phys. Soc. London* **1963**, *82*, 6–15.
33. Anoardo, E.; Galli, G.; Ferrante, G. Fast-Field-Cycling NMR: Applications and Instrumentation. *Appl. Magn. Reson*. **2001**, *20*, 365–404.
34. Kimmich, R.; Anoardo, E. Field-Cycling NMR Relaxometry. *Prog. Nucl. Magn. Reson. Spectrosc.* **2004**, *44*, 257–320.
35. Mittermaier, A.; Kay, L.E. Measurement of Methyl ^{2}H Quadrupolar Couplings in Oriented Proteins. How Uniform Is the Quadrupolar Coupling Constant? *J. Am. Chem. Soc*. **1999**, *121*, 10608–10613.
36. Burnett, L.H.; Muller, B.H. Deuteron Quadrupole Coupling Constants in Three Solid Deuterated Paraffin Hydrocarbons: C_2D_6, C_4D_{10}, C_6D_{14}. *J. Chem. Phys*. **1971**, *55*, 5829–5831.
37. Bloom, M.; Davis, J.H.; Valic, M.I. Spectral Distortion Effects Due to Finite Pulse Widths in Deuterium Nuclear Magnetic Resonance Spectroscopy. *Can. J. Phys*. **1980**, *58*, 1510–1517.
38. Kuebler, S.C.; Schaefer, D.J.; Boeffel, C.; Pawelzik, U.; Spiess, H.W. 2D Exchange NMR Investigation of the α-Relaxation in Poly(ethyl methacrylate) as Compared to Poly(methyl methacrylate). *Macromolecules* **1997**, *30*, 6597–6609.

39. Körber, T.; Mohamed, F.; Hofmann, M.; Lichtinger, A.; Willner, L.; Rössler, E.A. The Nature of Secondary Relaxations: The Case of Poly(ethylene-alt-propylene) Studied by Dielectric and Deuteron NMR Spectroscopy. *Macromolecules* **2017**, *50*, 1554–1568.
40. Litvinov, V.M.; Macho, V.; Spiess, H.W. Molecular Motions in Crystalline and Mesomorphic Forms of Poly(diethylsiloxane). *Acta Polymer.* **1997**, *48*, 471–477.
41. Lin, W.-Y.; Blum, F.D. Segmental Dynamics of Bulk Adsorbed Poly(methyl acrylate)-d_3 by Deuterium NMR: Effect of Adsorbed Amount. *Macromolecules* **1997**, *30*, 5331–5338.
42. Maddumaarachchi, M.; Mathota Arachchige, Y.L.N.; Zhang, T.; Blum, F.D. Dynamics of Cetyltrimethylammonium Bromide Head Groups in Bulk by Solid-State Deuterium NMR Spectroscopy. *Langmuir* **2018**, *34*, 11058–11065.
43. Meirovitch, E.; Liang, Z.; Freed, J.H. Protein Dynamics in the Solid State from ^{2}H NMR Line Shape Analysis: A Consistent Perspective. *J. Phys. Chem. B* **2015**, *119*, 2857–2868.
44. Metin, B.; Blum, F.D. Molecular Mass and Dynamics of Poly(methyl acrylate) in the Glass-Transition Region. *J. Chem. Phys*. **2006**, *124*, 054908.
45. Nambiar, R.R.; Blum, F.D. Segmental Dynamics of Bulky Poly(vinyl acetate)-d_3 by Solid State ^{2}H NMR: Effect of Small Molecule Plasticizer. *Macromolecules* **2008**, *41*, 9837–9845.
46. Vogel, M.; Rössler, E.A. Slow β Process in Simple Organic Glass Formers Studied by One and Two Dimensional ^{2}H Nuclear Magnetic Resonance. II. Discussion of Motional Models. *J. Chem. Phys*. **2001**, *115*, 10883–10891.
47. Bock, D.; Kalhau, R.; Micko, B.; Pötzschner, B.; Schneider, G.J.; Rössler, E.A. On the Cooperative Nature of the β-Process in Neat and Binary Glasses: A Dielectric and Nuclear Magnetic Resonance Spectroscopy Study. *J. Chem. Phys*. **2013**, *139*, 064508.
48. Vogel, M.; Rössler, E.A. Effects of Various Types of Molecular Dynamics on 1D and 2D ^{2}H NMR Studied by Random Walk Simulations. *J. Magn. Reson*. **2000**, *147*, 43–58.
49. Papon, A.; Saalwächter, K.; Schäler, K.; Guy, L.; Lequeux, F.; Montes, H. Low-Field NMR Investigations of Nanocomposites: Polymer Dynamics and Network Effects. *Macromolecules* **2011**, *44*, 913–922.
50. Litvinov, V.M.; Penning, J.P. Phase Composition and Molecular Mobility in Nylon 6 Fibers as Studied by Proton NMR Transverse Magnetization Relaxation. *Macromol. Chem. Phys.* **2004**, *205*, 1721–1734.
51. Abragam, A. *Principles of Nuclear Magnetism*; Oxford University Press: Oxford, UK, 1961.
52. Anderson, P.W.; Weiss, P.R. Exchange Narrowing in Paramagnetic Resonance. *Rev. Mod. Phys.* **1953**, *25*, 269–276.
53. Kehr, M.; Fatkullin, N.; Kimmich, R. Molecular Diffusion on a Time Scale Between Nano- and Milliseconds probed by Field-Cycling NMR Relaxometry of Intermolecular Dipolar interactions: Application to Polymer Melts. *J. Chem. Phys*. **2007**, *126*, 094903.
54. Kehr, M.; Fatkullin, N.; Kimmich, R. Deuteron and Proton Spin-Lattice Relaxation Dispersion of Polymer Melts: Intrasegment, Intrachain, and Interchain Contributions. *J. Chem. Phys*. **2007**, *127*, 084911.
55. Kariyo, S.; Stapf, S.; Blümich, B. Site Specific Proton and Deuteron NMR Relaxation Dispersion in Selectively Deuterated Polyisoprene Melts. *Macromol. Chem. Phys*. **2005**, *206*, 1292–1299.